

Shape-Shifting Technology of High-Molecular-Weight Hyaluronic Acid Realizing Youthful Skin

Fujii, Yoshimura, Mika^{1*}; Okishima, Anna¹; Ichiwata, Shimizu, Hiroko¹;

Onoue, Masatoshi¹; Oka, Takashi¹; Ashida, Yutaka²; Hara, Eijiro²

¹ MIRAI Technology Institute, Shiseido Co., Ltd., Yokohama, Japan

² Brand Value R&D Institute, Shiseido Co., Ltd., Yokohama, Japan

* Mika Yoshimura Fujii, 1-2-11 Takashima, Nishi-ku, Yokohama 220-0011, Japan, Tel.: +81-45-222-1600, Email: mika.fujii@shiseido.com

Abstract

Introduction: Hyaluronic acid (HA) is essential to maintain youthful skin. However, the level of HA in the epidermis diminishes with aging. This study was established to develop novel technology that delivers high-molecular-weight HA (HMW-HA) to the epidermis without reducing its original functions to realize youthful skin.

Methods: The size of HA was evaluated by multi-angle light scattering, partial specific volume, and molecular dynamics simulations. The amount of HA penetration was evaluated by the tape-stripping and cross-sectional observation of skin. The efficacy of the proposed technology was evaluated by measuring the softness and transparency of stratum corneum (SC), water retention capacity of HA, SC water content, and skin surface contours.

Results: It is difficult to achieve the skin penetration of HMW-HA without reducing its structure and properties. We demonstrated that HA shrank with the addition of magnesium chloride and that this shrunken HMW-HA showed drastic increases in HA penetration to the epidermis. In addition, the softness and transparency of SC were improved. Moreover, it was revealed that the addition of sodium metaphosphate expanded the overall volume of the shrunken HA. Combining this expansion method with shrunken HA achieved a fine and uniform skin texture because of restoration of HA's original water retention capacity.

Conclusion: The shape-shifting technology made it possible not only to provide the highest reported levels of HMW-HA to the epidermis, but also to regenerate its original water retention capacity and volume. This technology can supply natural HMW-HA non-invasively as a promoter of youthful skin in daily care.

Key Words: Hyaluronic Acid; Shape Control; Skin Penetration; Moisturizing

Introduction

Bio-based innovations are currently a major growth area and have markedly influenced the cosmetics industry. The global organic personal care market is expected to reach USD 42.19 billion by 2030, registering a compound annual growth rate of 9.1% during the forecast period [1]. This demand is driven by consumers who want to avoid problematic chemicals and are interested in products that contain natural ingredients. Methods that do not change the skin with artificial chemicals but instead enhance the original skin functions with bio-active ingredients need to be proposed as innovative solutions for cosmetics.

Hyaluronic acid (HA) is a naturally occurring biopolymer that can be manufactured by a microbial fermentation method. It is essential for maintaining youthful skin because it is involved in many biological processes, such as cell proliferation, cell migration, and cell differentiation [2, 3]. Because the level of HA in the epidermis diminishes with aging [4], providing additional HA as a trigger for biological processes can maintain and enhance the skin's original functions. However, HA shows low skin permeability and is ineffective when introduced to the skin through non-invasive methods because of its high molecular weight (HMW). Because of this, low-molecular-weight (LMW) HA is also utilized in cosmetics because of its higher penetration capacity than HMW-HA [5]. On the other hand, the biological efficacy differs between HMW- and LMW-HA. HMW-HA has anti-inflammatory and angiogenesis-inhibiting effects [6, 7], but LMW-HA has the opposite effects [8]. Moreover, HMW-HA has greater water retention capacity than LMW-HA [9]. Accordingly, HMW-HA that penetrates to the epidermis is expected to regenerate the function of skin with diminished HA. Meanwhile, the half-life of HA in the skin is extremely short (approximately 1 day). Thus, to maintain youthful skin, there is a need to develop methods for providing HA in daily care.

The particulation of HMW-HA, such as by the poly-ion complex method [10] or the solid-in-oil method [11], has been reported to increase the skin penetration of HMW-HA for cosmetic purposes. Meanwhile, particulation inhibits the binding between functional groups of HA and water despite carboxy groups and hydroxyl groups in HA having an important role of hydration. Therefore, achieving the skin penetration of HMW-HA with its original water retention capacity and structure is difficult. Injecting HA can provide HMW-HA or crosslinked-HA into the dermis and/or subcutaneous tissue topically, but it is painful and cannot provide HA to the whole face. Recently, microneedles have been reported to supply HA into the epidermis [12], but such needles

can also not be applied to the whole face.

The purpose of this study is to realize youthful skin using not artificial chemicals, but bio-active ingredients that enhance the skin's original function. We attempt to develop a novel technology that delivers HMW-HA to the epidermis without diminishing its original function and can be applied to the whole face as a daily cosmetic.

Materials and methods

Materials

Sodium hyaluronate [BIO-HYALURO 12 (NA), Shiseido] with an average molecular weight of 1100–1600 kDa was used as HMW-HA. Sodium metaphosphate (sodium hexametaphosphate, Kokusan Chemical, abbreviated as SMP), sodium chloride (Junsei Chemical, abbreviated as NaCl), potassium chloride (Fujifilm Wako, abbreviated as KCl), magnesium chloride hexahydrate (Fujifilm Wako, abbreviated as MgCl₂), calcium chloride dihydrate (Fujifilm Wako, abbreviated as CaCl₂), and aluminum chloride hexahydrate (Fujifilm Wako, abbreviated as AlCl₃) were used as reagents as purchased. As a solvent, deionized water was used in all experiments.

Skin penetration of HA to SC

Ex vivo human skin was used as a membrane and a diffusion cell array system (Introtec, Fig. 1a) was used as a test device. HA at 0.5 w/w% with each salt solution (0.14 Eq. of metal ions) was applied to the skin surface. The skin surface was set at 32±2°C. After 6 h, the skin was removed from the cell and washed with soap and purified water. The stratum corneum (SC) was then stripped by tape stripping (TS) 10 times. Six to ten tapes were extracted with 5 v/v% methanol solution.

Skin penetration of fluorescein amine-labeled HA

Here, 0.5 w/w% fluorescein amine (FA)-labeled HA solution with or without MgCl₂ was applied to the *ex vivo* human skin surface. After 6 h, the skin surface was washed and then embedded in OCT compound, and cryosections were made using a cryostat (CM3050S, Leica). The skin sections were observed using a fluorescence microscope (BX51, Olympus). In addition, the surface of the SC after wiping with water was observed with a microscope (LSM880, Zeiss).

Radius of gyration

The radius of gyration (R_g) of HA in the presence of MgCl₂ was evaluated by gel permeation chromatography (GPC)-multi-angle light scattering (MALS; Dawn

Heleos ii, Wyatt Technology). Various concentrations of MgCl₂ solution were used for the mobile phase, and measurements were carried out after filtration through a 0.45 µm cellulose acetate cartridge filter.

Molecular dynamics simulation

Molecular dynamics (MD) simulations were performed for 200 ns using GROMACS 2019.3. MgCl₂ was added to the system of 8 units of HA and water molecules. Glycam06g.itp and SPC/E were used as HA and water models, respectively [13]. The concentrations of MgCl₂ were set as 0 and 50 mM.

Rheology of SC sheet

The SC sheets were prepared with reference to the thermal trypsin treatment method [14]. After applying each sample, the sheets were dried overnight in a desiccator. DVA-220 (IT Measurement Control) was used to measure the dynamic viscoelasticity of SC sheets. The detected stress signal was converted into a dynamic storage elastic modulus (E') at 32°C and 50% relative humidity.

Transparency of SC sheet

An SC sheet was pasted on the plate and immersed in each sample solution at room temperature. After 24 h, the sheet was taken out and washed with deionized water. It was then dried at room temperature for 24 h and its transmission of visible light was measured with a haze meter (Murakami Color Research Laboratory).

Partial specific volume

Density measurements were performed at 20.00 ± 0.01°C on a DMA 4500 density meter (Anton Paar). The density increment ($\partial\rho/\partial w_{HA}$) was calculated from six separate density measurements of 0.1 w/w%–0.5 w/w% of HA solutions and the solvent.

The specific volumes of HA were calculated from equation (1) [15]:

$$v_{sp,HA}^0 = \lim_{w_{HA} \rightarrow 0} \frac{1}{\rho} \left[1 - \frac{1 - w_{HA}}{\rho} \frac{\partial \rho}{\partial w_{HA}} \right] \quad (1)$$

where ρ is the density of HA solution and w_{HA} is the mass of HA in the solution.

Differential scanning calorimetry

DSC TA2000 (Mettler–Toledo International) was used as the thermal analyzer. The

heating rate was set to 5°C/min in the range of -30°C to 30°C. Each measured sample had a mass of 5 mg. The water content was calculated from equations (2) and (3) [16]:

$$W_{nf} = W_t \left(\frac{w}{W} \% \right) - \frac{Q_{endo}}{Q_f} \times 100 \quad (2)$$

$$W_{HAb} = W_{sb} - W_{vb} \quad (3)$$

where W_{nf} is the content of non-freezing bound water (w/w%), W_t is the total water content (w/w%), Q_{endo} is the melting enthalpy of free water in samples (J/g), Q_f is the melting enthalpy of ice (experimental value, J/g), W_{HAb} is the amount of bound water near HA molecules (w/w%), W_{sb} is the bound water content of HA solution (w/w%), and W_{vb} is the bound water content of vehicle (w/w%).

***In vivo* skin efficacy test**

The insides of both forearms of the 6 women in our panel aged 20–49 years were washed with soap. The water content in the SC was measured using a probe (Corneometer® CM825, COURAGE + KHAZAKA) connected to a Corneometer® (Multiprobe MPA5, COURAGE + KHAZAKA). Six minutes after applying 0.5 w/w% HA with or without MgCl₂, the same amount of SMP solution or deionized water was applied. Ninety minutes later, the water content was measured without washing the measurement area. Changes in water content were calculated from the difference between the value after 90 min and that prior to application.

The 22 men in our panel aged 25–39 years washed their faces with soap. Then, anisotropy of skin furrows (VC1), proportion of skin furrows (ALL), average length of skin furrows (LEN), average width of skin furrows (WD), and number of skin ridges (SMA) [17] were measured using a digital microscope (Skin Vismom III, Shiseido). The men in the panel applied 0.5 w/w% HA with MgCl₂ solution (HA-Mg) in the night and the same amount of 0.03 w/w% SMP solution or water in the morning. The morning samples were randomly allocated to their right or left of faces. HA-Mg, SMP solution, and water samples contained 1 w/w% ethanol and 0.5 w/w% phenoxyethanol. The night sample was applied to the whole face, while the morning sample was applied to half the face after washing. After 4 weeks, the skin surface was measured again by the digital microscope.

Healthy volunteers were enrolled in these experiments after they had provided written informed consent. These protocols for human studies were approved by Shiseido Research Ethics Committee (Yokohama, Japan).

Statistics

Statistical analysis was performed using Statcel4 add-in software of Excel. Indicated *P*-values from multiple comparison tests were derived from Tukey's and Tukey–Kramer comparison tests. Student's *t*-test was conducted to compare the skin texture between the groups. Outliers were detected by the Smirnov–Grubbs test.

Results

Effect of ions on the skin penetration of HA

The penetration of HA with various salts is shown in Fig. 1b. The amount of HA from tape stripping 6–10 times was drastically enhanced by MgCl₂ compared with those with HA solution and other salts. Aggregation was observed in HA solution with AlCl₃. Next, the penetration of FA-labeled HA was observed by fluorescence microscopy (Fig. 1c and d). Fluorescence derived from FA-labeled HA was observed at the upper area of viable epidermis (VED) co-existing with MgCl₂ (Fig. 1d). Meanwhile, it was not observed for FA-labeled HA solution alone (Fig. 1c). These results showed that the

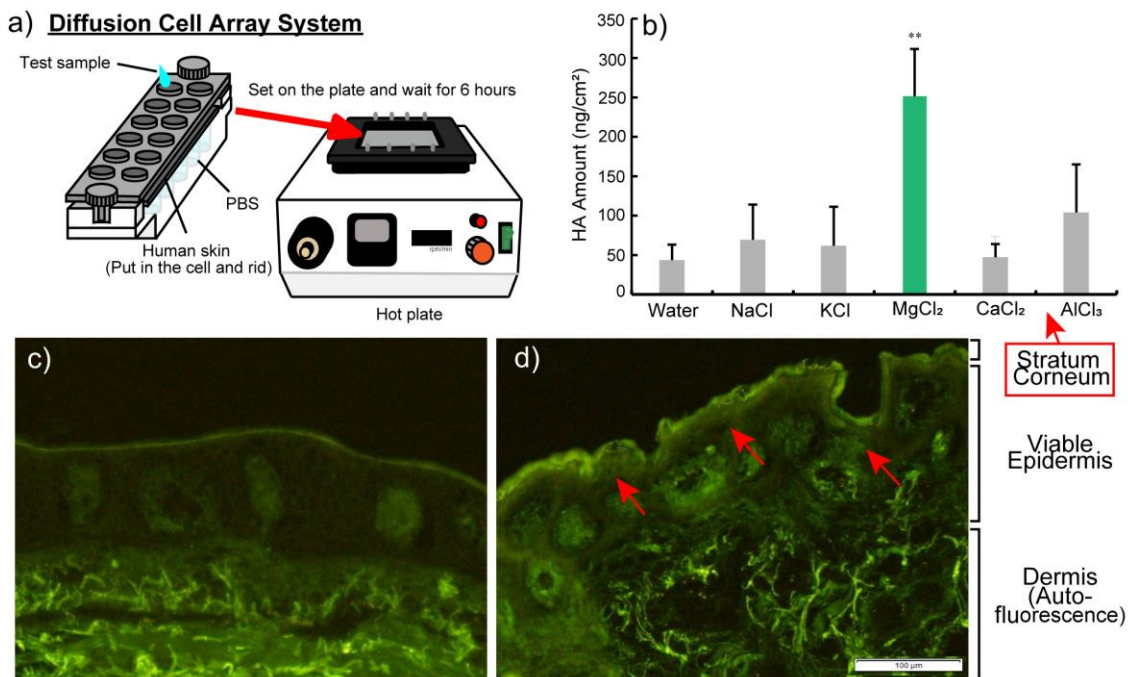


Figure 1 HA penetration test on *ex vivo* human skin. The test protocol using diffusion cell array system (a). HA amount is from tape stripping performed 6–10 times on stratum corneum 6 h after application (b) obtained from a Caucasian male in his 60s. Mean and S.D. are shown (*n*=3–4). **: *P* < 0.01 between HA with MgCl₂ and HA without/with other salts as determined by Tukey–Kramer comparison tests. Observation of skin cross section on 0.5 w/w% of FA-labeled HA solution (c) and 0.5 w/w% of FA-labeled HA with MgCl₂ (d) 6 h after application. Scale bars indicate 100 μ m. Fluorescence derived from FA-labeled HA was observed at the upper area of viable epidermis co-existing with MgCl₂.

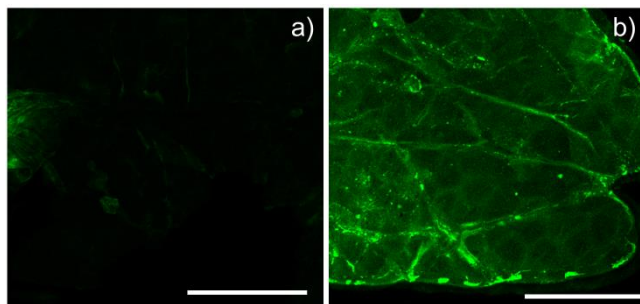


Figure 2 Skin surface fluorescence image.
Fluorescence image of SC surface on 0.5 w/w% of FA-labeled HA solution (a) and 0.5 w/w% of FA-labeled HA with $MgCl_2$ (b) 6 h after application. Scale bars indicate 50 μm . These images were taken from the top of SC after wiping the SC surface with water.

Table 1 Rgs of HA in $MgCl_2$ aqueous solution at each ionic strength.

Ionic Strength	Rg (nm)
0.01	127.8
0.05	115.4
0.1	103.3

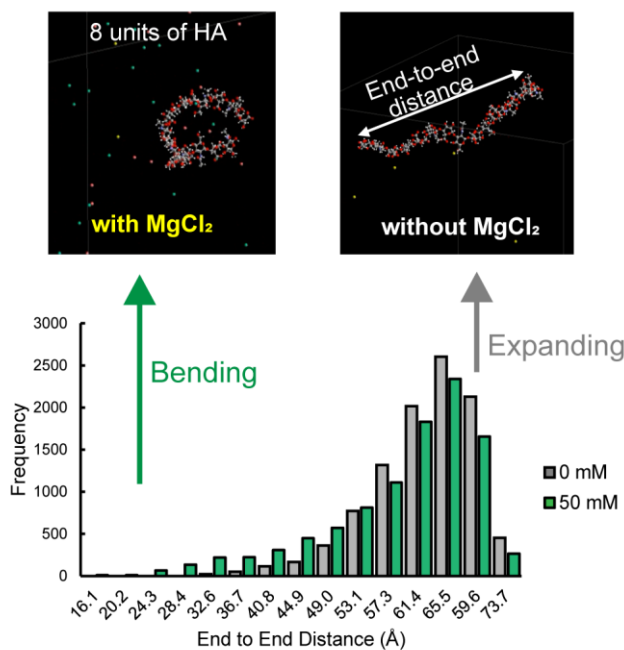


Figure 3 End-to-end distances of 8 units of HA with and without $MgCl_2$ by MD simulations.

HMW-HA was delivered to VED upon the addition of $MgCl_2$.

Observation of the SC surface after applying samples is shown Fig. 2. Little fluorescence was observed from the SC surface applied with FA-labeled HA, but strong fluorescence was detected from the SC surface and the intercellular spaces for FA-labeled HA with $MgCl_2$.

Effect of ions on the molecular size of HA

First, the Rgs were measured to evaluate the changes of the molecular size of HA upon adding $MgCl_2$. The Rgs of HA in various ionic strengths of $MgCl_2$ are shown in Table 1. The Rgs of HA decreased with increasing ionic strength of $MgCl_2$. Next, the end-to-end distance of 8 units of HA with and without $MgCl_2$ was calculated by MD simulation (Fig. 3). The proportion of end-to-end distances in the range of 20–40 Å was higher upon adding $MgCl_2$ than without $MgCl_2$, also showing that the HA chain was bent and shrunken by $MgCl_2$.

Softness and transparency of the SC by shrunken HA

To reveal the skin efficacy of shrunken HA (HA-Mg, shown in

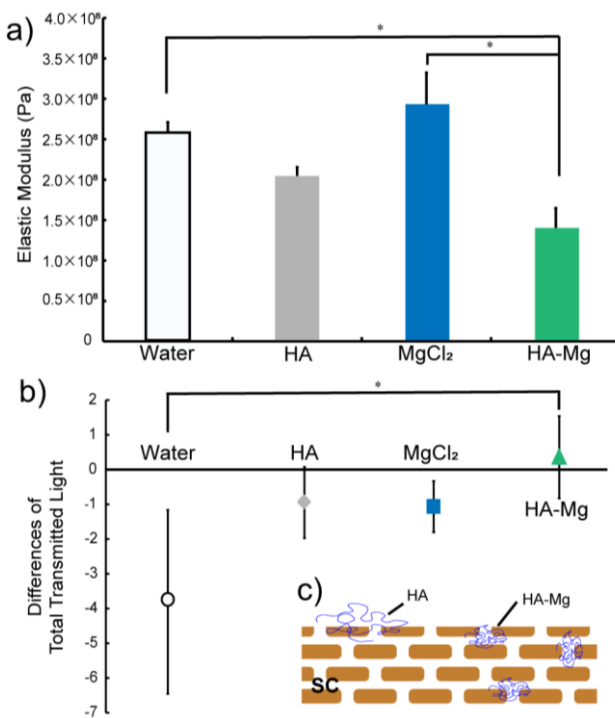


Figure 4 Effect of HA-Mg on SC sheet. Elastic modulus of SC sheet (a). Values are expressed as mean \pm S.D. (n=3). *: $P < 0.05$, Tukey's test. Water: no addition of any salts, HA: 0.1 w/w% HA solution, MgCl₂: MgCl₂ solution at 0.14 Eq. of the metal ions, HA-Mg: 0.1 w/w% HA with MgCl₂ at 0.14 Eq. of the metal ions. The differences of total transmitted light from SC sheet (b). Values are expressed as mean \pm S.D. (n=3–4). *: $P < 0.05$, Tukey-Kramer comparison tests. Water: no addition of any salts, HA: 0.5 w/w% HA solution, MgCl₂: MgCl₂ solution at 0.14 Eq. of the metal ions, HA-Mg: 0.5 w/w% HA with MgCl₂ at 0.14 Eq. of the metal ions. Illustration of the differences between HA and HA-Mg on SC (c).

Table 1 and Fig. 3), the dynamic storage elastic modulus (E') and the transmitted visible light of *ex vivo* SC were evaluated. First, the E' of SC applied with each sample is shown in Fig. 4a. HA-Mg significantly improved the E' of SC relative to water and MgCl₂ aqueous solution, showing that SC was softened by HA-Mg. The softness of SC associated with HA-Mg was greater than that for HA aqueous solution. Next, the differences in the transmission of visible light from SC between before and after the application of each sample were determined, as shown in Fig. 4b. Visible light transmission from SC decreased with the application of water, MgCl₂ aqueous solution, and HA aqueous solution. Meanwhile, the SC applied with HA-Mg showed no reduction in transmission and was much more transparent than that applied with water.

Expansion of the volume of shrunken HA by SMP

The partial specific volumes of HA-Mg and HA-Mg with SMP, a chelating agent, are shown in Table 2. MgCl₂ decreased the partial specific volume of HA, which corresponds to the reduction in the molecular size of HA shown in Table 1. When SMP was added to HA-Mg, the partial specific volume of HA increased to the same level as before adding MgCl₂.

Boosting by SMP of the moisturizing efficacy of shrunken HA

First, to reveal the water retention capacity of HA, HA-Mg, and HA-Mg with

Table 2 Partial specific volume of HA solution.

	Partial Specific Volume (cm ³ /g)
HA aqueous solution	0.60
HA aqueous solution with MgCl ₂	0.52
HA aqueous solution with MgCl ₂ and SMP	0.62

The concentrations of MgCl₂ and SMP were set to 0.14 Eq. of metal ions and 0.03 w/w% SMP.

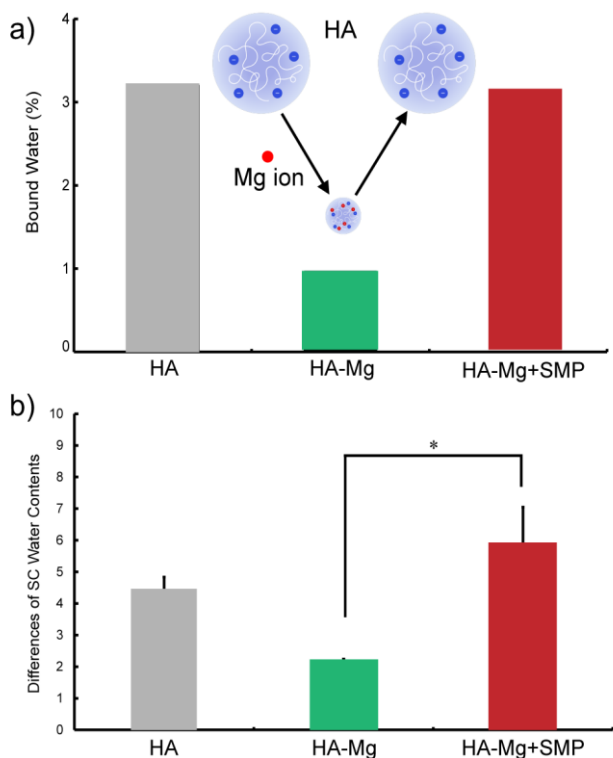


Figure 5 Effect of SMP on moisturizing efficacy of HA-Mg. Bound water contents of HA (a). Data represent mean values (n=3–5). Differences of water content 90 min after application (b). Data represent mean \pm S.E. (n=6). *: P < 0.05 between HA-Mg and HA-Mg + SMP as determined by Tukey's test. HA: HA solution, HA-Mg: HA with MgCl₂ at 0.14 Eq. of the metal ions, HA-Mg + SMP: combination between HA with MgCl₂ at 0.14 Eq. of the metal ions and 0.03 w/w% SMP.

SMP, the bound water was evaluated by differential scanning calorimetry (Fig. 5a). The bound water near HA was reduced upon adding MgCl₂, but it recovered with the addition of SMP to HA-Mg. Second, the differences of SC water content between before and after the application of each sample *in vivo* are shown in Fig. 5b. HA-Mg showed lower SC water content than HA aqueous solution, but this was also improved with SMP. The SC water content was not changed by SMP aqueous solution alone (data not shown). Finally, a 4-week *in vivo* continuous use test was conducted to demonstrate the efficacy of HA-Mg with SMP (Fig. 6). VC1, ALL, and SMA after 4 weeks of application of HA-Mg with SMP were better than those for HA-Mg alone. Meanwhile, LEN and WD did not differ between with and without SMP.

Discussion

There is increasing demand among consumers of cosmetics who want to avoid problematic chemicals and are interested in products that contain natural ingredients.

Methods that do not change the skin with artificial chemicals but instead enhance the original skin functions via bio-active ingredients need to be proposed as innovative solutions for cosmetics. HA is one of the best bio-active ingredients because it is essential for maintaining youthful skin given its involvement in many biological processes. Because the level of HA in the epidermis diminishes with aging [4], providing additional HA as a trigger for biological processes can maintain and enhance the skin's original functions. However, HA shows low skin permeability and is ineffective when introduced to the skin through non-invasive methods because of its high HMW. Moreover, the half-life of HA in the skin is extremely short; thus, to maintain youthful skin, there is a need to develop methods for providing HA in daily care. To proposal an innovative form of daily skin care, we attempted to develop a novel technology that delivers HMW-HA to the epidermis without diminishing its original function and can be applied to the whole face as a daily cosmetic.

The size of HA was reduced and its skin penetration was enhanced by the addition of MgCl₂ (Table 1, Fig. 1 and Fig. 3). HA molecules would shrink when exposed to metal ions such as magnesium ions because the repulsion between carboxylate anions would be inhibited and the HA flexion frequencies would be increased by neutralization of the negative charge in HA. This compacting efficacy of MgCl₂ is also suggested to become the driving force for the penetration of HA. In addition, the neutralization of negative charge in HA is considered to promote the partition of HA to the skin. Recently, domains with an abundance and dearth of lamellar and lateral packing in SC intercellular lipids have been reported [18], and the domain with a dearth is considered to partly contribute to the penetration of HMW compounds. HA nanoparticles prepared by the poly-ion complex method are known to penetrate from intercellular spaces of SC in its upper area [19]. We also investigated the proportion of HA-Mg that penetrates to SC via the intercellular route because strong fluorescence derived from FA-labeled HA was observed from intercellular spaces from the SC surface after applying shrunken HA (Fig. 2). Moreover, the transappendageal pathway is known as one of the routes by which nanoparticles can penetrate the skin [20]. Smaller-sized particles can also more easily penetrate the skin. HA-Mg is smaller than HA alone (Table 1), so these pathways could also contribute to the permeability of HA-Mg. MgCl₂ showed higher efficacy for promoting the penetration of HA relative to other salts (Fig. 1). The Rg of HA-Mg was smaller than those with other salts (data not shown). In addition, MgCl₂ has high deliquescence and less precipitation, which would also enhance the penetration of HA at a finite dose. Accordingly, compaction of HA and deliquescence properties of MgCl₂ would be key points of our technology for promoting HMW-HA penetration (shrunken

HA).

This shrunken HA improved the softness and transparency of SC (Fig. 4). Aged SC is known to harden and develop wrinkles because of the increasing difference in softness relative to the underlying dermis with aging [21, 22]. Penetrated HA in the form of HA-Mg would contribute to the softness of SC because HA has excess bound water [15] and is expected to improve the elasticity gap in aged skin. The disruption of the orientation of SC keratin decreases the transmission of visible light, so the evaporation rate of SC water is important for a proper orientation [24]. It is likely that penetrated HA improves the transparency of SC by inhibiting the evaporation rate of water there, as well as improving the orientation of keratin. From these results, shrunken HA was revealed to enable the penetration of HMW-HA into the skin and to improve skin softness and transparency. Meanwhile, the bound water near HA was reduced in HA solution upon the addition of MgCl₂ (Fig. 5a). Moreover, SC water content upon the treatment of HA solution with MgCl₂ was also decreased compared with that with HA alone (Fig. 5b). The carboxylate anion plays an important role in the water retention capacity of HA, so these reductions could be attributed to the shielding of carboxylate anion. From these results, the regeneration of shrunken HA function would be necessary to maximize the moisturizing capacity of original HA.

The method of restoring shrunken HA is presented in Table 2, Fig. 5 and Fig. 6. The compacted partial specific volume of HA-Mg was increased by adding SMP (Table 2). This result shows that the SMP re-expands the volume of HA reduced by MgCl₂. Magnesium ions reduce the HA volume by shielding carboxylate anions, but the chelating agent, SMP, forms a complex with the magnesium ions and these ions are separated from HA. The separation of magnesium ions from HA releases carboxylate anions, which could regenerate the repulsion between carboxylate anions and re-expand the volume of HA. This expansion by SMP was a specific phenomenon in MgCl₂ aqueous solution; it was not observed in NaCl aqueous solution (data not shown). It is likely that chelating agents work not monovalent metal ions but divalent metal ions. Moreover, the reductions of bound water in HA aqueous solution with MgCl₂ and water content of SC *in vivo* upon the treatment of HA-Mg were also recovered with SMP (Fig. 5). It was suggested that this occurred because SMP captured magnesium ions and carboxylate anions were re-released. Thus, SMP not only re-expands the volume of HA-Mg, but also recovers the original function of HA. There is a trade-off relationship between penetrating HA and keeping its moisturizing efficacy. This restoring technology solves this issue and has made possible the coexisting of HA penetration and moisturizing efficacy, which has not previously been achieved. The HA-Mg with SMP retained better

VC1, ALL, and SMA values than HA-Mg alone after a test involving 4 weeks of continuous use (Fig. 6). VC1, ALL, and SMA represent the anisotropy of skin furrows, the proportion of skin furrows, and the number of skin ridges; hence, a lower VC1 value, and higher ALL and SMA values reflect fine and uniform skin textures. Improving the bound water of HA-Mg and re-expanding the volume of HA-Mg with the addition of SMP on and in the skin would promote the skin texture after continuous use. Skin texture changes markedly with aging, with the size of ridges increasing and furrows of skin flowing in one direction [23]. It is suggested that the continuous use of the technology

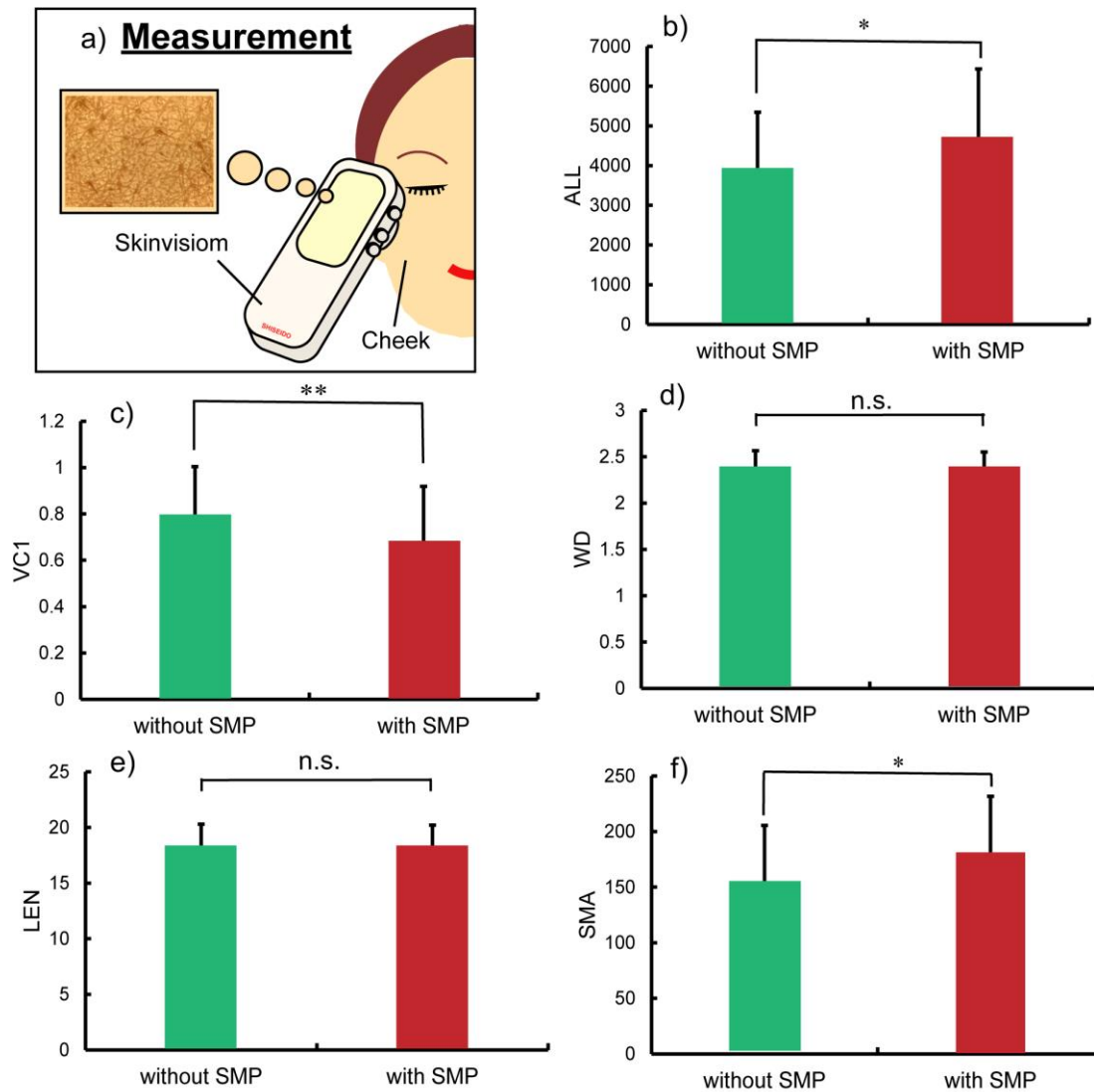


Figure 6 Skin textures 4 weeks after continuous use. The skin surface analyzer with a digital microscope was used on the top of the cheek before and after use of the samples (a). Proportion of skin furrows (ALL) (b), anisotropy of skin furrows (VC1) (c), average width of skin furrows (WD) (d), average length of skin furrows (LEN) (e), and number of skin ridges (SMA) (f) were collected from 22 Japanese males in their 20s to 30s. Data represent mean \pm S.D. (n=22). *: $P < 0.05$ between HA-Mg and HA-Mg + SMP as determined by Student's *t*-test.

proposed in this paper can realize a youthful skin texture because HA-Mg with SMP leads to a finer and more uniform skin texture than HA-Mg alone. This remarkable efficacy is obtained because SMP works to release carboxylate anions in HA and regenerates the original function of HA in the skin. Consequently, this shape-shifting method (Fig. 7) achieves soft and transparent skin, and a fine skin texture non-invasively without the use of artificial chemicals. HA works not only as a moisturizer but also as a trigger for youthful skin via its biological effects, so injecting HA into the epidermis without diminishing its original properties would become an advanced solution for aged skin. To date, the injection of HA has been an invasive procedure requiring aesthesia. Our technology can provide a new opportunity for consumers to introduce HA into the epidermis non-invasively in their daily care.

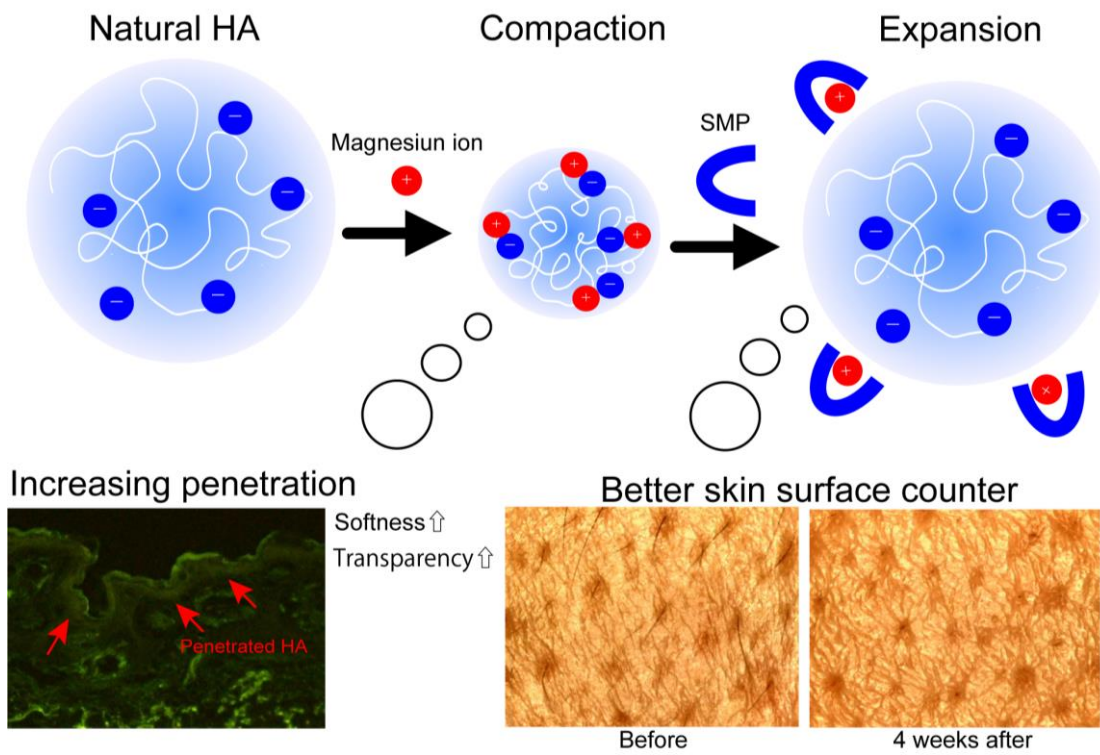


Figure 7 Illustration of shape-shifting technology.

Conclusion

In this study, we developed compaction and expansion methods for the shape-shifting of HMW-HA (Fig. 7). The compaction method drastically increased the skin penetration of HA and improved the softness and transparency of SC. Magnesium ions were revealed to play an important role in this compaction by neutralizing the carbohydrate anions of HA. Meanwhile, the expansion method allowed shrunken HA to

return to a larger size and recover its original water retention capacity. This recovery effect of SMP conferred a fine and uniform skin texture resembling younger skin. This shape-shifting technology made it possible to maintain a balance between the penetration and efficacy of HA and succeed in maximizing the original functions of HA. This technology is strongly expected to be used for advanced cosmetics in which HA can be introduced into the epidermis on the whole of the face non-invasively, which is important given that the level of HA diminishes in the epidermis with aging. This approach enables natural HA as a trigger for youthful skin to be applied to the epidermis without using anesthesia or invasive methods. Consequently, this approach is a solution to meet the expectations of consumers who hope to enhance their skin function using bio-active ingredients.

Acknowledgments

We would like to thank Dr. Atsushi Sogabe and Ms. Ayano Nakamura for useful discussions, and Dr. Yotaro Morishima for helpful advice on the MALS measurements. We are also grateful to Mr. Seiji Nishikawa and Mr. Koutaro Takada for test sample preparation, and Mr. Junya Hiyoshi, Mr. Naoki Saito, Mr. Taiki Kazama, Ms. Megumi Mizugaki and Dr. Kumiko Kikuchi for support with the *in vivo* human test.

Conflict of Interest Statement

NONE

References

1. Organic Personal Care Market Worth \$42.19 Billion By 2030 (grandviewresearch.com)
2. Bourguignon LYW, Ramez M, Gilad E, Singleton A, et al (2006) Hyaluronan-CD44 interaction stimulates keratinocyte differentiation, lamellar body formation/secretion, and permeability barrier homeostasis. *J Invest Dermatol* 126: 1356–1365.
3. Bourguignon LYW, Singleton PA, Diedrich F (2004) Hyaluronan-CD44 interaction with Rac1-dependent PKN-g kinase promotes PLC γ 1activation, Ca $^{2+}$ signaling and cortactin-cytoskeleton function leading to keratinocyte adhesion and differentiation. *J Biol Chem* 279: 29654–29669.
4. Iriyama S, Nishikawa S, Hosoi J, et al (2010) Basement membrane helps maintain epidermal hyaluronan content. *Am J Pathol*, 191: 1010–1017.
5. Smejkalova D, Huerta-Angeles G, Ehlova T (2015) Hyaluronan (Hyaluronic Acid):

- a natural moisturizer for skin care. Harry's 9th Edition (2) Part 4.1.3: 605–622.
- 6. Bollyky PL, Lord JD, Masewicz SA, et al (2007) High molecular weight hyaluronan promotes the suppressive effects of CD4+ CD25+ regulatory T cell. *J Immunol* 179: 744–747.
 - 7. Tempel C, Gilead A, Neeman M (2000) Hyaluronic acid as anti-angiogenic shield in the preovulatory rat follicle. *Biol Reprod* 63: 134–140.
 - 8. Kage M, Tokudome Y, Matsunaga Y, et al (2014) Effect of hyaluronan tetrasaccharides on epidermal differentiation in normal human epidermal keratinocytes. *Int J Cosmet Sci* 36: 109–115.
 - 9. Průšová A, Šmejkalová D, Chytil M, et al (2010) An alternative DSC approach to study hydration of hyaluronan. *Carbohydr Polym* 82: 498–503.
 - 10. Tokudome Y, Komi T, Omata A, et al (2018) A new strategy for the passive skin delivery of nanoparticulate, high molecular weight hyaluronic acid prepared by a polyion complex method. *Sci Rep* 8: 2336.
 - 11. Funatsu A, Tahara Y, Yamanaka S, et al (2011) Oil gel sheets utilizing solid-in-oil technique. *MEMBRANE* 36: 57–62.
 - 12. Matsunaga Y, Fujiwara S, Mori Y, et al (2012) Development of self-dissolving microneedles consisting of hyaluronic acid as an anti-wrinkle treatment. *IFSCC Magazine* 2: 73–78.
 - 13. Vuorio J, Vattulainen I, Martinez-Seara H (2017) Atomistic fingerprint of hyaluronan–CD44 binding. *PLOS Comput Biol* 13: e1005663
 - 14. Kilgman AM, Christphers E (1963) Preparation of isolated sheets of stratum corneum. *Arch Dermatol* 88: 702–705.
 - 15. Kargerová A, Pekař M (2014) Densitometry and ultrasound velocimetry of hyaluronan solutions in water and in sodium chloride solution. *Carbohydr Polym* 106: 453–459.
 - 16. Kim SJ, Lee CK, Kim SI (2004) Characterization of the water state of hyaluronic acid and poly (vinyl alcohol) interpenetrating polymer networks. *J Appl Polym Sci* 92, 1467–1472.
 - 17. Takahashi M (1994) Image analysis of skin contour. *Acta Derm Venereol (Stockh)* 185: 9–14.
 - 18. Suzuki T, Uchino T, Hatta I, et al (2018) Evaluation of the molecular lipid organization in millimeter sized stratum corneum by synchrotron X-ray diffraction. *Skin Res Technol* 24: 621–629.
 - 19. Shigefuji M, Tokudome Y (2020) Nanoparticulation of hyaluronic acid: A new skin penetration enhancing polyion complex formulation: Mechanism and future

- potential. Materia 14: 100879.
- 20. Rancan F, Gao Q, Graf C, et al (2012) Skin penetration and cellular uptake of amorphous silica nanoparticles with variable size, surface functionalization, and colloidal stability. ACS Nano 6 (8): 6829–6842.
 - 21. Christensen MS, Hargens CW 3rd, Nacht S, et al (1977) Viscoelastic properties of intact human skin: instrumentation, hydration effects, and the contribution of the stratum corneum. J Invest Dermatol 69:282-2866.
 - 22. Ogura, Y, Hara, T, Ninomiya, M, et al (2020) Emergence of Eye Wrinkles Can Be Controlled By Balancing The Elasticity of The Stratum Corneum and The Dermis.31th IFSCC Congress in press.
 - 23. Lagarde JM, Rouvrais C, Black D (2005) Topography and anisotropy of the skin surface with ageing. Skin Res Tech 11: 110–119.
 - 24. Iwai I, Kunizawa N, Yagi E, et al (2013) Stratum corneum drying drives vertical compression and lipid organization and improves barrier function *in vitro*. Acta Derm Venereol 93: 138–143.